

# Population pyramids yield accurate estimates of total fertility rates \*

**Mathew E. Hauer** <sup>1\*</sup> *University of Georgia*  
**Carl P. Schmertmann** <sup>2,3</sup> *Florida State University*

---

Recent methodological advances in indirect migration and mortality estimation<sup>1,2,3</sup> reveal important unforeseen patterns underlying these population processes, yet accurate indirect estimation of fertility remains difficult. The primary fertility index for a population, the total fertility rate (TFR), requires data on births disaggregated by mother's age and thus cannot be calculated for the many areas and time periods that lack such information. Here we discuss a universal methodological framework for estimating TFR using inputs as minimal as the age-sex structure of a population. We show that the implied total fertility rate (iTFR) accurately estimates fertility from a population's age-sex structure in a wide range of scales, time periods, and even species. We also discuss two extensions of the iTFR that offer improved accuracy with minimal additional data requirements. To demonstrate the utility of this approach, we produce the first complete county-level map of U.S. fertility, reconstruct historical TFRs for 1000 additional country-years up to 150 years prior to the collection of birth records, and estimate TFR for the U.S. conditioned on household income, a variable unrecorded on U.S. birth records. Given its parameter-free nature, the method has wide applicability across space and time. We anticipate that our methodological framework will allow extension of fertility analysis to new sub-populations, time periods, and geographies, expanding our ability to understand fertility processes.

---

\* Corresponding author. hauer@uga.edu. p: 706-542-9369.

<sup>1</sup> Carl Vinson Institute of Government, University of Georgia. 201 N. Milledge Ave. Athens, GA USA 30602.

<sup>2</sup> Department of Economics, Florida State University.

<sup>3</sup> Center for Demography and Population Health, Florida State University.

---

\*The data and code that supports this analysis are available in the supplementary materials. The authors would also like to thank A. Bronikowski, R. Lawler, and S. Alberts for their assistance with the nonhuman data; and B. Jaroz and K. Devivo for feedback on earlier versions. Thanks y'all!

## Main Text

Fertility is the primary engine of global population change<sup>4</sup> and is linked to the United Nation’s Sustainable Development Goals for female education, child and maternal mortality, gender equality, and reproductive health<sup>5</sup>. The total fertility rate (TFR; the expected number of children born over a complete reproductive lifetime) is a critical component of population change, and scientists and practitioners use it in a wide range of applications<sup>6,7,8,9,10,11,12,13,14,15</sup>.

Although the conventional technique for calculating TFR is straightforward, it requires data on births disaggregated by age of mother. This makes TFR incalculable in: (i) countries and regions that lack detailed birth records, (ii) historical populations without vital event registration, such as the United States prior to 1933, (iii) small-area populations for which reporting agencies mask birth records for privacy reasons, and (iv) any subpopulation not identified on official birth records, such as the women in a specific income decile, religion, tribe, or caste. The need for disaggregation of births by mother’s age thus limits fertility analysis mainly to large populations in contemporary countries with good vital registration systems.

Numerous indirect estimation techniques have been proposed to circumvent these limitations<sup>16,17,18</sup>. These methods are often regression-based, and they rely on covariates – such as mean age at marriage, percent of women ever married, etc. – that may be absent from census data and therefore must be collected in surveys. The resulting scale- and time-dependent estimates are often inaccurate<sup>19,20</sup>, subject to coefficient drift, and like TFR they are limited to areas, time periods, and populations with sufficiently detailed data.

Here we discuss a modeling framework that overcomes these problems and demonstrate the near-universal applicability of a parameter-free estimation method. The method uses census or survey counts of population by age and sex, commonly called *age pyramids*. Its principles are straightforward and well known. Recent research has demonstrated that errors

for this method tend to be smaller than other regression-based methods<sup>20</sup> and that minor modifications using commonly-available data can further improve the estimates.<sup>21</sup>

The foundation of our approach is the relationship between the number of young children in a population, the overall fertility level, child mortality, and relative fertility by age. Demographic calculations in the *Supplementary Material* show that the expected number of children,  $C$ , below age five in a population is the product of four factors:

$$C = W \cdot p \cdot s \cdot TFR \tag{1}$$

where  $W$  is the total number of reproductive-age women (usually ages 15-49 for humans),  $p$  is the average proportion of lifetime fertility experienced by those women over the previous five years [measured in  $(births\ in\ last\ 5\ years)/(lifetime\ births)$ ],  $s$  is the expected fraction of surviving children born in the past five years [ $(surviving\ children\ under\ five)/(births\ in\ last\ 5\ years)$ ], and  $TFR$  is the expected number of children born per complete reproductive lifetime [ $(lifetime\ births)/woman$ ].

We construct three alternative TFR estimators from equation (1), each requiring slightly more input data than the last. The first two variants rely on reorganizing equation (1) as an expression for TFR:

$$TFR = \frac{1}{s} \cdot \frac{1}{p} \cdot \frac{C}{W} \tag{2}$$

in which total fertility is the product of the child/woman ratio, a child mortality multiplier  $\frac{1}{s}$ , and an age structure multiplier  $\frac{1}{p}$ .

The simplest approximation to equation (2) assumes that child mortality is close to zero ( $s \approx 1$ ), and that women are uniformly distributed over 35 years of reproductive ages

( $p \approx 1/7$ , so that the age structure multiplier is approximately 7). Following Hauer et al.<sup>20</sup> we call the resulting estimator the *implied total fertility rate* (*iTFR*):

$$iTFR = 7 \cdot \frac{C}{W}. \quad (3)$$

A second variant uses additional information from the age-sex pyramid to improve the approximation of the  $\frac{1}{p}$  term in equation (2). In the *Supplementary Material* we show that this multiplier is a decreasing function of the proportion of of reproductive-age women between ages 25 and 34 (denoted  $\pi_{25-34}$ ), and that  $\frac{1}{p} \approx 10.65 - 12.55 \pi_{25-34}$  is an excellent approximation for human populations. Replacing  $p = \frac{1}{7}$  in equation (3) with that approximation produces our second estimator, which we call the *extended TFR* or *xTFR*

$$xTFR = (10.65 - 12.55 \pi_{25-34}) \cdot \frac{C}{W} \quad (4)$$

This estimator adjusts for non-uniform distributions of women within reproductive ages. For any given child-woman ratio, *xTFR* produces a lower estimate for lifetime fertility if women are concentrated in high-fertility ages.

Our third TFR estimator is Bayesian. It exploits additional details from the age-sex pyramid about female age structure within reproductive ages, and it requires one additional demographic index from an external source: an estimate of under-five mortality. The Bayesian approach treats the number of children in equation (1) as a Poisson random variable, and uses prior distributions for parameters  $p$  and  $s$ , derived from patterns observed in large demographic databases<sup>22,23</sup>. We define the *BayesTFR* estimator as the median of the marginal posterior distribution of a population's *TFR*, conditional on  $C$  and  $W$  observed in the age-sex pyramid. Because they are probabilistic, *BayesTFR* estimators automatically produce uncertainty measures and point estimates.

We evaluate the accuracy of the three derivations using data from the Human Fertility Database and Human Mortality Database<sup>22,23</sup> for nearly 1,800 fertility schedules between

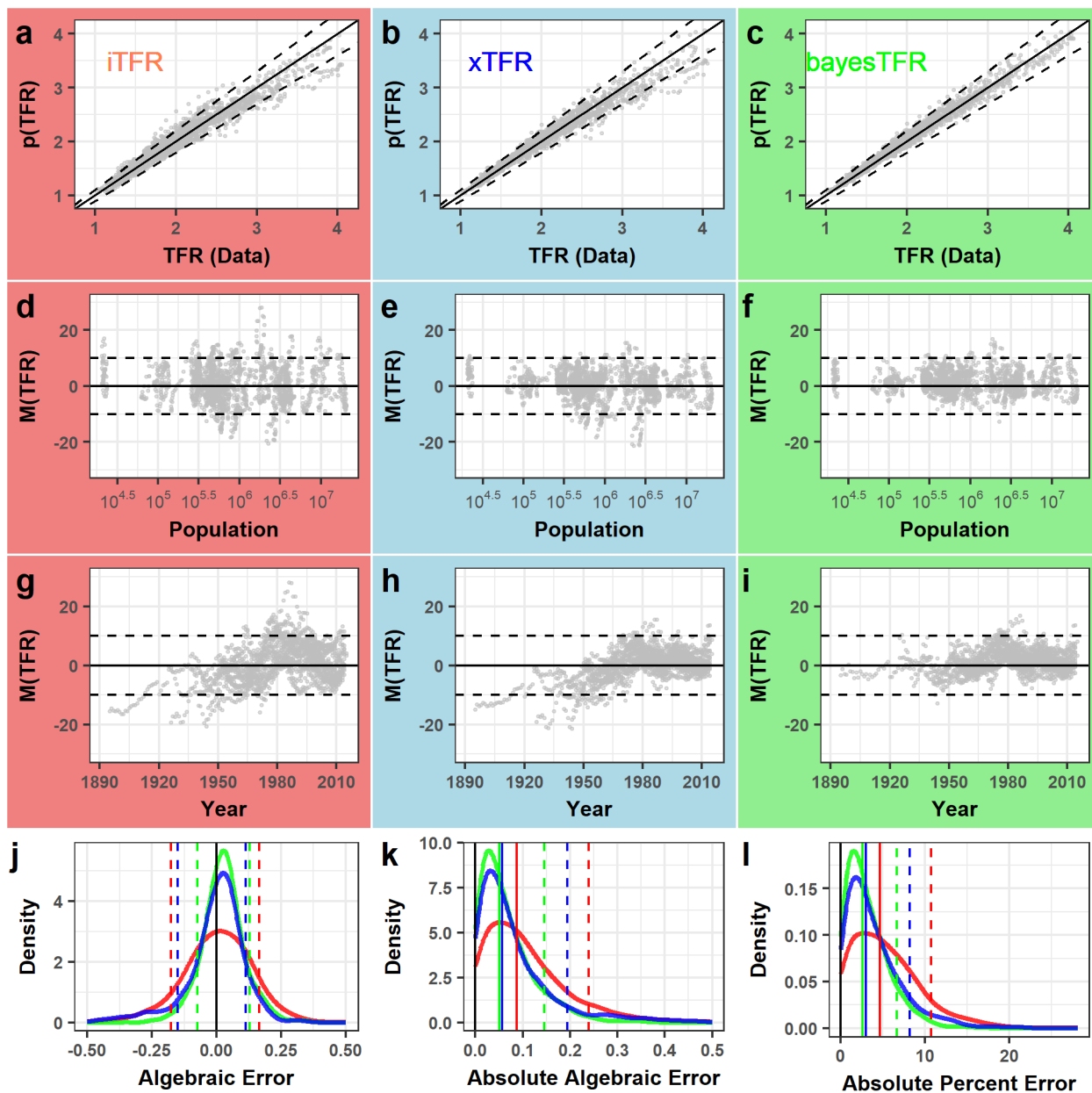


Figure 1: **Estimated TFR from Age-Sex Pyramids** We compare the performance of three estimators against observed total fertility rates. (a, d, g) in the first column use *iTFR*; (b, e, h) in the second column use *xTFR*; (c, f, i) in the third column use *BayesTFR*. (a, b, c) display scatters of estimated TFR against the observed 5-year average TFR from schedules in the Human Fertility Database for 1891-2015. The solid line is  $Y = X$ , and the dashed lines are  $Y = 0.90X$  and  $Y = 1.10X$ . (d, e, f) illustrate percent error,  $M(TFR) = 100 \cdot (1 - \text{observation}/\text{estimate})$ , for each method against population size. The dashed lines represent errors of  $\pm 10\%$ . (g, h, i) plot percent errors,  $M(TFR)$  against the year in which the age-sex pyramid is observed. (j) plots the distribution of algebraic errors for each method. The dashed lines correspond to the 10th and 90th percentile errors for each method. (k) plots the distribution of absolute algebraic errors. (l) plots the distribution of absolute percent errors colored for each method (*iTFR*=red, *xTFR*=blue, *bayesTFR*=green). The solid lines correspond to the 50th percentile error, and the dashed lines correspond to the 90th percentile errors colored for each method. Regardless of formulation, estimates are accurate over many scales and times.

1891 and 2015 across 30 countries (see Table 2 in the *Supplementary Materials* for a complete list). This dataset comprises only complete, official vital event statistics and is the most complete and accurate collection of observed fertility data compiled to date (Figure 1). We find good agreement between estimated and observed TFRs for all three methods (Fig. 1, a, b, c). We include an additional analysis of the errors associated with the United Nation’s more heterogeneous fertility estimates<sup>24</sup> (n= 2,613) and find similarly low error rates as with the HMD/HFD observed data. Due to the UN fertility estimates being *estimates* rather than observations, we have included the UN evaluation in the *Supplementary Material* (Figure 5 and Table 4).

Demographic estimators are typically more accurate for larger populations (due to the law of large numbers) and for more recent time periods (due to improved data collection practices). However, we find that error rates are independent of population size (Fig. 1, d, e, f) and do not vary across time (Fig. 1, g, h, i), suggesting scale and temporal independence uncommon in other indirect methods.

Even the simplest and least accurate of the three variants, *iTFR*, predicts the total fertility rate with absolute errors of less than 0.09 births/woman in half of the HFD populations, and less than 0.24 births/woman in 90% (Table 1). Absolute percent errors for *iTFR* are also quite small relative to most indirect demographic estimators: 50% of errors are within  $\pm 4.62\%$  of the true *TFR*, and 90% are within  $\pm 10.75\%$ . As shown in Figure 1 and Table 1, the additional information contained in the *xTFR* and *BayesTFR* estimators produce even lower error rates. In short, we find that for national populations in countries with accurate data and (mostly) low mortality, *TFR* estimates from age-sex pyramids are a significant improvement over previous indirect estimation methods<sup>20,19</sup>.

To test the generalizability of the method, we examine the accuracy of the implied fertility derivation in 11 nonhuman populations (nine primate species, one lion species, and one seal species) (Figure 2)<sup>32,25,29,30,31,27,28</sup>. These populations vary substantially in population size and fertility patterns, allowing us to assess whether the method works across species and

Table 1: **Summary statistics for the three estimators using data from the HFD and HMD.** APE is the Absolute Percent Error. All methods produce TFR estimates with median errors of less than 1/10th of a birth.

Method	50th Percentile Absolute Error	90th Percentile Absolute Error	50th Percentile APE	90th Percentile APE
iTFR	0.09	0.24	4.6%	10.7%
xTFR	0.06	0.19	3%	8.2%
BayesTFR	0.05	0.15	2.6%	6.6%

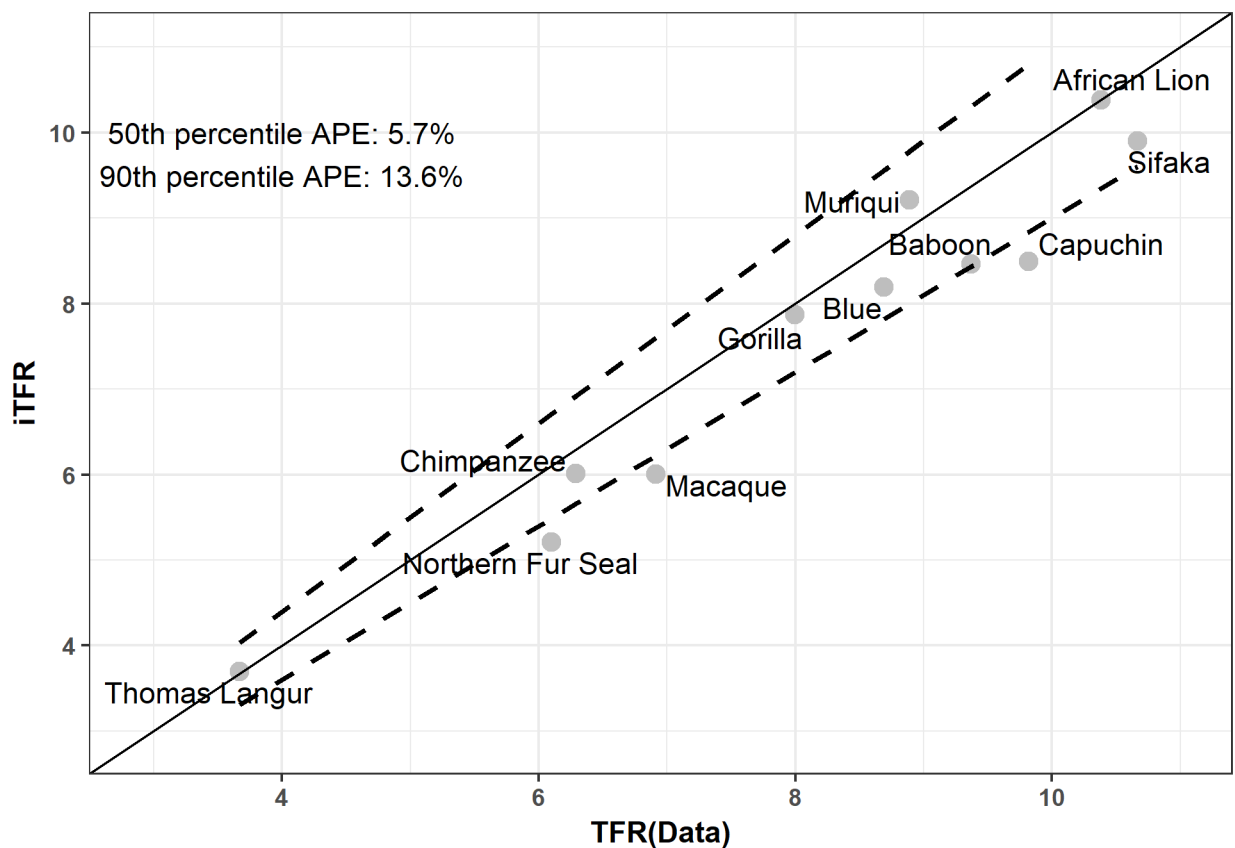


Figure 2: **iTFR using nonhuman Fertility Data.** We test the iTFR using data from eight wild and one captive primate species<sup>25,26,27,28</sup>, one wild lion species<sup>29,30</sup>, and one wild seal species<sup>31</sup>. These species exhibit markedly different menarche and menopause, length of fertility schedule, and fertility tempo from each other and from humans. We plot the observed TFR against the estimated TFR using the iTFR formulation. The solid line is  $Y=X$ , and the dashed lines represent  $\pm 10\%$  of  $Y=X$ . Overall the iTFR performs remarkably well across the 11 nonhuman species, losing very little accuracy for species with markedly different fertility characteristics.

varying fertility patterns. In contrast to humans, for whom scientists typically demarcate menarche and menopause at ages 15 and 50 years, respectively, menarche among the eleven species ranges from a low of age 2 for Sifakas (*Propithecus verreauxi*) and African lions (*Panthera leo*) to a high of 11 years for Chimpanzees (*Pan troglodytes*). Reproductive age spans range from a low of 7 years for Thomas Langurs (*Presbytis thomasi*) to a high of 38 years for Chimpanzees. These species display reproductive age spans, fertility schedules, and TFRs that differ greatly from humans. We find that  $iTFR$  accurately estimates total fertility among these species (**Figure 2**). Remarkably, this simple method with limited data requirements can accurately estimate total fertility across multiple species with minimal loss of accuracy compared to human populations (**Table 1** and **Table 4**). These results with nonhuman species suggest the method captures fundamental properties that govern fertility and that it can nearly universally be applied to a wide span of previously inestimable populations, time periods, geographies, and possibly species.

Accurate estimation of  $TFR$  from age-sex pyramids greatly expands our ability to estimate fertility across varying geographies, time periods, and subpopulations. The three panel plots in (**Figure 3**) demonstrate the flexibility of the method. For privacy reasons, the National Center for Health Statistics does not publish fertility information for US Counties with populations fewer than 100,000. As a result, sub-national county-level  $TFR$  can be calculated in only 500 of the approximately 3000 US Counties, significantly hindering the examination of sub-national fertility patterns. Here we use age-sex data from the 2010 US Census to produce  $xTFR$  estimates for all US counties, creating the first complete county-level map of US fertility (**Fig. 3, a**) and report the low error associated with these counties using coefficients derived from the HFD/HMD (50th percentile APE = 3.3%, **Table 3**).

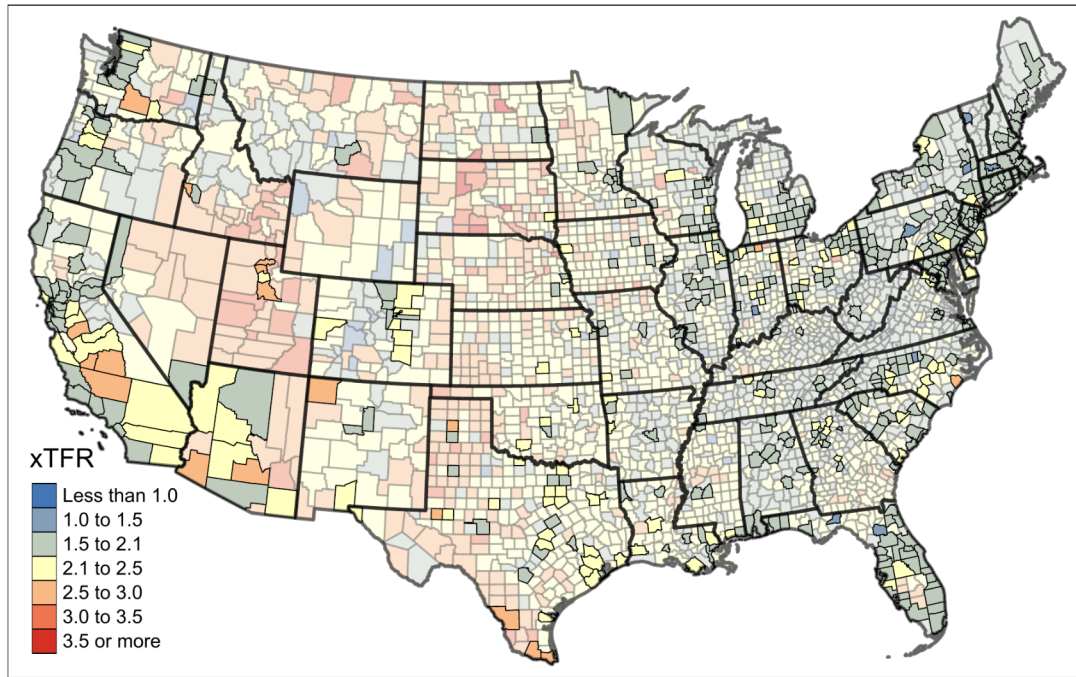
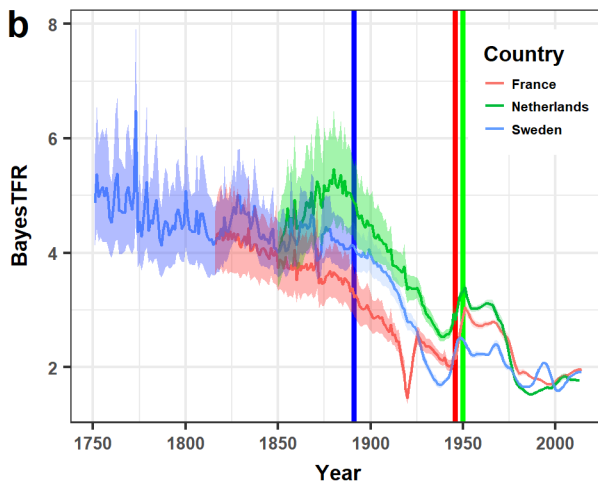
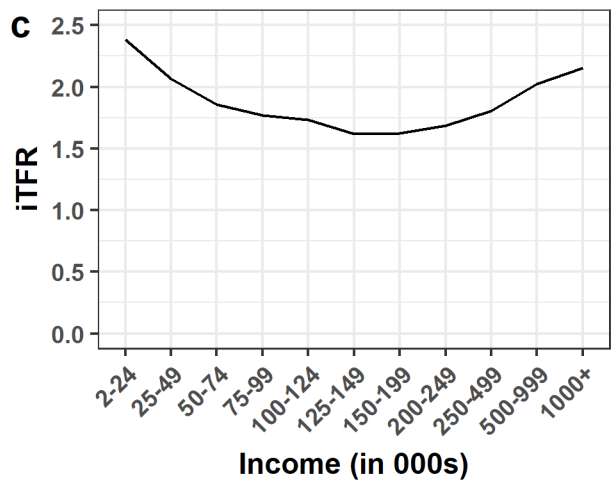
We also extend our analysis of the Human Mortality Database by producing fertility estimates for all 2955 country-years of data in the HMD (an additional 1000 country-years' of estimates prior to the collection of birth records) but highlight our findings for three example countries: Sweden, France, and the Netherlands (**Fig. 3, b**). Sweden began

tabulating the detailed birth records necessary for  $TFR$  calculation in 1891, France in 1946, and the Netherlands 1950. However, these countries collected both mortality and age-sex data considerably earlier (1751 for Sweden, 1816 for France, 1850 for the Netherlands). By using the *BayesTFR* method, we can reconstruct historical TFRs to create a time series of fertility data well before birth record collection began, significantly improving our ability to explore historical fertility patterns from up to 250 years ago.

In (**Fig. 3, c**) we use the basic *iTFR* method to estimate TFRs by household income level in the United States, using data on the age-sex composition of households in different income strata from the US Census Bureau’s American Community Survey (ACS). By linking age-sex data to household income, we are able to produce estimates of TFR by income groups, subpopulations for which fertility levels were previously unavailable.

Researchers can tailor their *iTFR* formulation to the data available or the research question due to the flexible data requirements, a rare feature in methodologies, and can do so with confidence in the accuracy of the resultant estimates. As we show in **Figure 3**, the applications of such a robust, simple method cannot be understated. The implied fertility rate opens the door for sophisticated fertility analyses in many previously inestimable populations of interest to sociologists<sup>9</sup>, economists<sup>33</sup>, anthropologists<sup>34</sup>, epidemiologists<sup>35</sup>, historians<sup>36</sup>, and population geographers<sup>37</sup>. The parameter-free, scale-, time-, and species-robust technique can estimate fertility rates even in areas where such data are not collected systematically as it relies only on age-sex data – ubiquitous basic data collected in censuses across scale and time.

We anticipate this method will open new lines of inquiry into human fertility patterns. The global demographic transition is typically examined post-1950<sup>38</sup>; however, using age-sex structure data, researchers can examine the global demographic transition in greater detail farther back in time. Similarly, recreations of historic human fertility rates rely on estimates of energy balance and the relative metabolic load or a universal density-dependent demographic model, amongst others<sup>39</sup>. Using the methods proposed here, anthropologists

**a****b****c**

**Figure 3: Revealing latent fertility patterns.** We demonstrate that the *iTFR* framework can be used in a variety of situations. (a) uses the *xTFR* method to estimate total fertility rates in US Counties based on Census 2010 data. The National Center for Health Statistics masks fertility data for counties with fewer than 100,000 people for privacy reasons making fertility estimates possible for only 524 of the approximately 3000 US counties. The darker counties are the counties with actual fertility data. (b) uses the *BayesTFR* method to estimate historic fertility rates in three European countries using data from the Human Mortality Database. The vertical lines correspond to when birth registration began in each country. The shaded regions represent the 90th percentile. (c) uses the *iTFR* method on household income data from the Census Bureau’s American Community Survey. Birth registration is not recorded by income group, but we are able to estimate fertility rates using household survey data. These three examples represent previously inestimable populations by geography, time period, and sub-population and demonstrate the methodological flexibility of the *iTFR* framework.

could recreate historic human fertility rates directly from ancient censuses, such as from the ancient Rome<sup>40</sup>, while accounting for underenumeration and child-mortality. Finally, there is now increased demand for high-resolution gridded population datasets for climate change research<sup>41,42</sup>. Because our methods work well for small populations, scientists could use them to estimate small-area fertility levels and changes, as inputs to gridded population projections or to gridded fertility level datasets.

### *Competing Interests*

The authors declare that they have no competing financial interests.

Table 2: Human Fertility Database Countries and years of data availability.

Country	Data Avail. (# years)	Country	Data Avail. (# years)
Austria	1951-2014 (64)	Netherlands	1950-2012 (63)
Belarus	1964-2014 (51)	Norway	1967-2014 (48)
Bulgaria	1947-2009 (63)	Portugal	1940-2015 (76)
Canada	1921-2011 (91)	Russian Federation	1959-2014 (56)
Chile	1992-2005 (14)	Slovakia	1950-2009 (60)
Czech Republic	1950-2014 (65)	Slovenia	1983-2014 (32)
Estonia	1959-2013 (55)	Spain	1922-2014 (93)
Finland	1939-2015 (77)	Sweden	1891-2014 (124)
France	1946-2013 (68)	Switzerland	1932-2014 (83)
Germany	1990-2013 (24)	Taiwan	1976-2014 (39)
Hungary	1950-2014 (65)	Ukraine	1959-2013 (55)
Iceland	1960-2010 (51)	England & Wales	1938-2013 (76)
Italy	1954-2012 (59)	Scotland	1945-2013 (69)
Japan	1947-2014 (68)	Northern Ireland	1974-2013 (40)
Lithuania	1959-2013 (55)	United States of America	1933-2014 (82)

## Supplementary Information

*Data:*

**Human Fertility Database.** Data on fertility patterns comes from the Human Fertility Database<sup>22</sup>, the most complete and accurate historical patterns of human fertility currently available. Age-specific fertility rates are entirely based on official vital statistics and are not modeled. The HFD covers fertility schedules for 34 countries between 1891 and 2015, containing 1,870 country-years of age-specific and total fertility rates.

**Human Mortality Database.** Data on mortality rates comes from the Human Mortality Database<sup>23</sup>, the most complete and accurate historical patterns of human mortality currently available. Mortality rates come from official death counts from vital statistics, census counts, birth counts, and population estimates from varying sources. The  $q(5)$  values and population counts used in our analysis were gathered from this data source.

**Nonhuman data.** Primate age-specific fertility data for seven species come from Bronikowski et al<sup>25,26</sup>. This dataset contains female age-specific fertility estimates for seven wild primates: sifaka (*Propithecus verreauxi*) in Madagascar, muriqui (*Brachyteles hypoxanthus*) in Brazil;

capuchin (*Cebus capucinus*) in Costa Rica; baboon (*Papio cynocephalus*) and blue monkey (*Cercopithecus mitis*) in Kenya; chimpanzee (*Pan troglodytes*) in Tanzania; and gorilla (*Gorilla beringei*) in Rwanda. The primate species were continuously monitored for at least 29 years.

Thomas langur (*Presbytis thomasi*) data come from Wich et al<sup>28</sup>. These data were collected at the Ketambe Research Station, Leuser Ecosystem, Sumatra, Indonesia between 1987 and 2000. We use the age-data taken from Table II to estimate the iTFR and use data from the DATLife database<sup>43</sup> for the observed TFR.

Southern pig-tailed macaque (*Macaca nemestrina*) data come from Ha et al<sup>27</sup>. These data were collected at the largest captive-bred colony of pig-tailed macaque's in existence at the Animal Records System at the University of Washington's Regional Primate Research Center (WaRPRC). These data reflect 30 years of records at the colony (1967-1996). We use the age-specific fertility rate data from Table I for the observed TFR and the animal-years variable in that same table for the iTFR. Animal-years refer to the number of animal years exposed to risk of fertility in age interval  $x$ .

Northern fur seal (*Callorhinus ursinus*) data come from Barlow and Boveng<sup>31</sup>. We use data from Table 1 for the age frequency ( $n_x$ ) to estimate iTFR and data on the birth rate ( $B_x$ ) to calculate the TFR. These data were estimated from female seals taken from 1958 to 1961.

African lion (*Panthera leo*) fertility data come from Packer et al<sup>30</sup> via Jones et al<sup>29</sup>. These data were collected in Serengeti National Park and Ngorongoro Crater, Tanzania since 1966 and 1962.

All non-human populations'  $\alpha$  and  $\beta$  were calculated as the maximum/minimum age groups with observed fertility information. The number of females were subsequently summed over the containing interval.

Table 3: Summary statistics for the  $xTFR$  and  $iTFR$  methods using US county level data from Census 2010. APE is the Absolute Percent Error. The counties with observed fertility data are outlined in **Fig. 3a**.

Method	n	50th percentile APE	90th percentile APE
$iTFR$	524	6.48%	12.77%
$xTFR$	524	3.3%	10.08%

**US Income Fertility.** Data for estimating US TFR conditioned on household income come from the US Census Bureau’s American Community Survey’s 5-year 2012-2016 estimates using Data Ferret.

**US County Fertility.** To estimate county-level fertility in the US we use two data sources. To produce  $xTFR$  and  $iTFR$  estimates we use age-sex distributions of county populations from the 2010 Decennial Census. We evaluate the accuracy of these estimates by comparing to published county-level data from the National Center for Health Statistics (NCHS), obtained via the Center for Disease Control (CDC)’s Wide Ranging Online Data for Epidemiological Research (WONDER) tool. For privacy reasons, NCHS suppresses fertility information for counties with fewer than 100,000 residents. Thus we can assess  $xTFR$  errors for only 524 of the 3,142 US counties and county equivalents.

**Table 3** reports the errors associated with both the  $iTFR$  and  $xTFR$  methods for US counties that also have corresponding observed total fertility rates. These errors are on par with the errors observed using the HMD/HFD data (see **Table 1**).

**Demographic Relationships between TFR and age-sex distributions.**

The period total fertility rate ( $TFR$ ) is the expected number of children born over a complete reproductive lifetime at current age-specific rates:

$$TFR = \int_{\alpha}^{\beta} f(a) da \tag{5}$$

where  $f(a)$  is the fertility rate (births per woman-year) at exact age  $a$  and  $[\alpha, \beta)$  is the reproductive age range (i.e., the set of ages with non-zero fertility rates). In practice researchers approximate  $f(a)$  with a step function that has a constant rate  $F_a$  within each

$n$ -year age interval  $[a, a + n)$ .  $F_a$  values are estimated as ratios of annual births to the mid-year population of women in each age group ( $F_a = \frac{B_a}{W_a}$ ).

TFR is then calculated as

$$TFR = n \cdot \sum_{a=\alpha}^{\beta-n} \frac{B_a}{W_a} \quad (6)$$

For human populations scientists commonly use  $(\alpha, \beta, n) = (15, 50, 5)$ . In that case there are seven age groups, with fertility rates  $F_{15}, F_{20}, \dots, F_{45}$ , and  $TFR = 5 \cdot \sum F_a$ .

Data for age-sex pyramids is also typically reported by age groups, commonly with  $n = 5$ . Analysis of relationships between  $TFR$  and the relative numbers of women and children by age group requires consideration of several demographic factors. First, not all children born during the previous  $n$  years will still be alive at the time the population is enumerated. Second, not all women who gave birth over the past  $n$  years will still be alive to be counted. Third, surviving women in a given  $n$ -year age group at the time of enumeration were only in that age group for a fraction of the past  $n$  years. For example, 30–34 year olds were 25–29 at the beginning of the five-year period preceding enumeration, and would have spent an average of approximately half of the last five years in the 25–29 age group.

These are all familiar considerations for scientists who do population projections. A slight rearrangement of standard cohort-component, Leslie matrix formulas<sup>44</sup> for age groups of width  $n = 5$  shows that the expected number of surviving children of both sexes, per surviving woman in age group  $[a, a + 5)$  (which we will call *age group a*) at the end of a five-year period is

$$\begin{aligned} C_a &= \left[ \frac{L_{a-5}}{L_a} \cdot F_{a-5} + F_a \right] \frac{L_0}{2} \\ &= TFR \cdot \frac{L_0}{5} \cdot \frac{1}{2} \left( \frac{L_{a-5}}{L_a} \cdot \phi_{a-5} + \phi_a \right) \\ &= TFR \cdot s \cdot p_a \end{aligned} \quad (7)$$

where  $\phi_a$  is the fraction of lifetime fertility occurring in age group  $a$  ( $5 \cdot F_a/TFR$ );  $L_a$  is expected person-years lived in age group  $a$ , in a life table with a radix  $l_0 = 1$ ;  $s$  is the expected fraction still alive among children born in the past five years ( $L_0/5$ );  $W_a$  is the observed women in age group  $a$ ; and  $W$  is the total number of women enumerated at childbearing ages [15, 50).

$C_a$  is the product of three multiplicative factors:  $TFR$ , child survival  $s$ , and an age-specific fertility proportion  $p_a$  that is an average of  $\phi_{a-5}$  and  $\phi_a$ , slightly weighted toward the lower age group to account for potential maternal mortality.

The expected total number of surviving 0-4 year olds is therefore

$$C = \sum_{a=15}^{45} W_a C_a = W \cdot p \cdot s \cdot TFR \quad (8)$$

where  $p = \frac{1}{W} \sum W_a p_a$  is the population-weighted mean of  $p_a$  values.

### **iTFR.**

We can rearrange equation (8) as an expression for TFR:

$$TFR = \frac{1}{s} \cdot \frac{1}{p} \cdot \frac{C}{W} \quad (9)$$

If women of childbearing ages are uniformly distributed across reproductive ages, then  $p = \frac{n}{\beta - \alpha}$  where  $n$  is the width of age groups. If also we assume near-zero child-mortality ( $s \approx 1$ ) over the first  $n$  years of life, then equation (9) further simplifies to

$$iTFR = \frac{\beta - \alpha}{n} \cdot \frac{C}{W} \quad (10)$$

For human populations divided into five-year age groups  $(\alpha, \beta, n) = (15, 50, 5)$  and  $iTFR = 7 \cdot \frac{C}{W}$ . For other species the  $\frac{C}{W}$  multiplier may differ.

### **xTFR.**

The  $iTFR$  formulation assumes that  $p = \frac{1}{7}$ , meaning that the women enumerated in the age-sex pyramid experienced a (mortality-adjusted) average of one-seventh of their lifetime

fertility over the previous five years. In practice this is not exactly true, due to possible concentrations of women in high- or low-fertility age groups. For example, if the age pyramid has a high concentration of women in their late 20s and early 30s, then typical age patterns of human fertility make it likely that they have just passed through five especially high-fertility ages and that  $p > \frac{1}{7}$ . Conversely, high concentrations of women 40–49 in the age pyramid would suggest  $p < \frac{1}{7}$ .

We examined 1,859 fertility schedules in the HFD for which the true  $TFR$  is known, and calculated the empirical values of  $TFR$  divided by the child-woman ratio – that is, we calculated the multipliers necessary to convert the child-woman ratio into the  $TFR$ . The  $iTFR$  formula assumes that these multipliers all equal seven. In the HFD we found that true multipliers ranged from a low of 4.52 (Taiwan 1986) to a high of 11.29 (France 1946, a very unusual post-war population). However, the correct multipliers are within 10% of the  $iTFR$  value (6.3–7.7) in 68.7% of the country-years, and 90% of HFD multipliers fall between 6.02 and 7.79.

Although the  $iTFR$  assumption would typically lead to small errors, it is possible to construct improved multipliers by examining patterns in the HFD data. In particular, multipliers should be negatively correlated with the proportion of women in high-fertility age groups. Knowledge of typical age patterns of human fertility suggests that in many populations women in their late 20s and early 30s are the most likely to have given birth over the previous five years, so that multipliers should be lower in populations with high concentrations of women 25–34.

We tested correlations between various measures of the age structure within female reproductive ages. As expected we observed a clear relationship between the proportion of women aged 25–34 ( $\pi_{25-34}$ ) and the multiplier (Figure S1.,  $R^2=0.388$ ). Using other age groups to predict the multiplier led to lower correlations ( $R^2$  using  $\pi_{15-24} = 0.163$ ,  $\pi_{20-29} = 0.349$ ,  $\pi_{25-34} = 0.388$ ,  $\pi_{30-39} = 0.179$ ,  $\pi_{35-44} = 0.108$ ,  $\pi_{40-49} = 0.096$ ). We then replaced the  $iTFR$  multiplier of seven with its predicted value from the regression:

$$xTFR = (10.65 - 12.55\pi_{25-34}) \cdot \frac{C}{W} \quad (11)$$

This formulation improves the estimates of total fertility (**Figure 1**, **Figure 5**, **Table 1**, **Table 3**, and **Table 4**) but requires additional information about the distribution of women in the fertility interval.

We tested another derivation of  $xTFR$  based on the proportions of women in every five-year age group,

$$xTFR = \left( \sum_a \hat{\beta}_a \pi_a \right) \cdot \frac{C}{W} \quad (12)$$

However, we found that using the population aged 25-34 produced almost identical estimates with minimal loss of accuracy.

### **Bayes TFR.**

We extend our previous approach into a Bayesian framework relating the number of children aged 0-4 to women aged 15-49. The  $iTFR$  formulation outlined in equation (10) does not account for the potential error associated with any of the given parameters. The  $xTFR$  incorporates additional information from the age structure to improve the estimates but does not account for infant mortality or possible estimation errors in the number of women of childbearing ages.  $s$  and  $p$  cannot not be truly known and could be subject to random errors in measurement.

We deconstruct the estimation of total fertility from equation (9) into  $TFR$ ,  $C$ ,  $W$ ,  $s$ , and  $p$  producing a five-parameter model with four of the parameters deriving from the age-structure –  $C$ ,  $W$ ,  $p$ , and  $TFR$ ). The fifth parameter,  $s$ , is not information embedded within the age structure and must be supplied in addition to the age structure. These parameters



Figure 4: Proportion of women aged 25-34 among women aged 15-49 against the ideal multipliers in the HFD/HMD data.

can be broadly categorized as fertility ( $TFR, p$ ), mortality ( $s$ ), and age structure ( $W$ ) with the result of these quantities being the expected number of surviving children ( $C$ ).

**Fertility Parameters.** We decompose the fertility schedule for 5-year age groups into two components: level and shape

$$(F_{10}, F_{15}, \dots, F_{45}) = \frac{TFR}{5} \cdot (0, \phi_{15}, \dots, \phi_{45}) \quad (13)$$

where  $TFR$  is the total fertility rate and  $\phi_a$  is the proportion of lifetime fertility that occurs in age group  $a$ . Fertility is negligible before age 15; thus,  $F_{10} = 0$ . The proportions  $\phi_{15} \dots \phi_{45}$  are rewritten into indices, such that  $\gamma_a = \ln(\frac{\phi_a}{\phi_{15}})$  for  $a = 15 \dots 45$  such that  $\phi_a(\gamma) = \frac{\exp(\gamma_a)}{\sum_z \exp(\gamma_z)}$  sum to one.

The  $\gamma$  indices are modelled as  $\gamma = m + X\beta$  where  $m$  and  $X$  are constants derived from empirical data (see below) and  $\beta$  are shape parameters. These three fertility parameters ( $TFR, \beta_1, \beta_2$ ) yield eight 5-year fertility rates ( $F_{10} \dots F_{45} : \beta \rightarrow \gamma \rightarrow \phi$  and  $\frac{TFR}{5} \cdot \phi = F$ ).

We use a completely uninformative, improper prior for  $TFR$ :  $f(TFR) \propto 1$ . We assign higher probability to more typical fertility patterns by building the prior for  $\beta$  coefficients from information in the HFD and the US Census Bureau's International Database<sup>45</sup> to create priors of the shape of the fertility schedule by age. We calculate  $\gamma$  indices for  $F_a$  empirical schedules (n=226 from the IDB, n=411 from the HFD), and then performed a singular value decomposition on the (de-meant) 6x637  $\gamma$  array. This produces a model in which each of the 637 columns of  $\gamma$  could be well approximated by the mean vector plus a weighted sum of two principal components:  $\gamma_i \approx m + X\beta_i$ . We scale the two columns of  $X$  so that  $\beta_i$  coefficients have zero means, unit variances, and zero covariances over the empirical data  $i = 1 \dots 637$ .

These calculations produce constants  $X = \begin{pmatrix} 0 & 0.27 & 0.54 & 0.73 & 0.88 & 1.04 & 1.52 \\ 0 & 0.32 & 0.51 & 0.51 & 0.35 & 0.05 & -0.72 \end{pmatrix}'$ , with

which we use the prior

$$\beta \sim N(0, I_2) \quad (14)$$

with support restricted to the range  $[-2,+2]$  for each  $\beta$  coefficient, in order to better mimic the HFD distributions. When we examine the  $X$  matrix, we find that  $\beta_1$  affects the mean age of childbearing and  $\beta_2$  affects the variance: If  $\beta_1$  is higher, fertility is postponed; if  $\beta_2$  is higher, fertility is concentrated in fewer age groups.

**Mortality Parameters.** We model child and adult mortality with a two-parameter relational mortality model<sup>46</sup>. The probability of death before age five ( $q_5$ ) and a shape parameter  $k$  with typical values between -2 and +2 index the mortality schedule. The model uses fixed constants  $\{a_x, b_x, c_x, v_x\}$  derived from mortality schedules in the Human Mortality Database:

$$\ln \mu_x(q_5, k) = a_x + b_x [\ln q_5] + c_x [\ln q_5]^2 + v_x k \quad , \quad x = 0, 1, 5, 10 \dots 45 \quad (15)$$

Mortality rates  $\mu_0$  and  $\mu_1$  refer to age intervals  $[0, 1)$  and  $[1, 5)$ ,  $\mu_x$  refers to 5-year age intervals  $[x, x + 5)$  for all other age groups.  $q_5 = 1 - l_5$  is a model parameter, meaning there are no  $\{a_x, b_x, c_x, v_x\}$  constants for calculating  $\mu_1$ ; instead,  $\mu_1$  is calculated by  $\mu_1 = -\frac{1}{4} [\mu_0 + \ln(1 - q_5)]$ .

We convert log mortality rates into life table person-years,  $L_a$ , for 5-year age intervals  $[a, a + 5)$  using standard demographic approximations. Survival probabilities to exact ages are  $l_0 = 1$ ,  $l_1 = e^{-\mu_0}$ ,  $l_5 = l_1 \cdot e^{-4\mu_1}$ , and  $l_x = l_{x-5} \cdot e^{-5\mu_{x-5}}$  for  $x = 10 \dots 45$ . Life table person-years are  $L_0 = \frac{1}{2}(l_0 + l_1) + \frac{4}{2}(l_1 + l_5)$  and  $L_a = \frac{5}{2}(l_a + l_{a+5})$  for  $a = 5 \dots 45$ . Thus the two mortality parameters ( $q_5, k$ ) yield 10  $L_a$  values ( $L_0, L_5 \dots L_{45}$ ).

To account for the uncertainty in the mortality estimates, we use a beta distribution of  $q_5$  (denoted as  $\hat{q}_5$ ). The prior is defined as

$$q_5 \sim Beta[a(\hat{q}_5), b(\hat{q}_5)] \quad (16)$$

where  $a(\hat{q}_5)$  and  $b(\hat{q}_5)$  are chosen so that  $P[q_5 < \frac{1}{2} \min(\hat{q}_5)] = P[q_5 > 2 \max(\hat{q}_5)] = .05$ . This assigns a 90% prior probability that under-five mortality  $q_5$  is between one-half and twice the observed  $q_5$  value.

For the shape parameter  $k$ , we use the prior

$$k \sim N(0, 1) \tag{17}$$

which centers the distribution at zero and has a low probability of falling out of the  $[-2, +2]$  range. We assume that mortality parameters  $q_5$  and  $k$  are independent.

The values for parameters  $(TFR, \beta, q_5, k)$  imply specific values  $K_a$  in equation (7). The expected number of children to the  $W_a$  women observed in age group  $a$  is  $W_a K_a$ , and the observed number of surviving children may be modeled as  $C_a \sim Poisson(W_a K_a)$ . It is reasonable to assume that  $C_a$  values are statistically independent, conditional on fertility and mortality rates, so that their sum  $C = \sum_a C_a$  is also a Poisson random variable. Thus,

$$C|W, TFR, \beta, q_5, k \sim Poisson \left[ \sum_{a=15}^{45} W_a K_a(TFR, \beta, q_5, k) \right] \tag{18}$$

**Posterior Distribution of TFR.** The posterior for parameters conditional on data is

$$P(TFR, \beta, q_5, k|C, W) \propto L(C|W, TFR, \beta, q_5, k) f_\beta(\beta) f_q(q_5) f_k(k) \tag{19}$$

where the likelihood on the right-hand side is the Poisson likelihood in equation (18), and the  $f$  functions represent the prior densities implied by equations (14), (16), and (17), respectively. Note that the improper flat prior for  $TFR$  does not affect the posterior distribution.

The marginal posterior for TFR, which expresses the relative probabilities of alternative fertility levels given the number of children  $C$  and the counts of women  $W_{15} \dots W_{45}$ , is

$$P(TFR|C, W) \propto \int L(C|W, TFR, \beta, q_5, k) f_\beta(\beta) f_q(q_5) f_k(k) d\beta dq_5 dk \tag{20}$$

Table 4: **Summary statistics for the three estimators using data from the United Nations.** APE is the Absolute Percent Error.

Method	n	50th Percentile Absolute Error	90th Percentile Absolute Error	50th Percentile APE	90th Percentile APE
iTFR	2613	0.23	1.23	6.8%	18.9%
xTFR	2613	0.25	1.26	6.7%	19.4%
BayesTFR	2613	0.17	0.67	4.4%	11.3%

In practice, we sample from the full posterior distribution in equation (19) by applying Markov Chain Monte Carlo (MCMC) methods. Specifically, we program the model in the *Stan* MCMC language<sup>47</sup>, as implemented in the *rstan* package in *R*<sup>48,49</sup>. We use the empirical density of the sampled *TFR* values to estimate the marginal posterior of *TFR* in equation (20).

## United Nations Fertility Analysis

The HFD/HMD data represent the most complete and accurate observed total fertility data available. However, these data primarily represent low-fertility, low-mortality country-years. It is possible, though unlikely, that our framework produces errors in excess of other methods in high-fertility, high-mortality country-years. Unfortunately no administrative datasets of the same quality as the HMD/HFD exist for many high-fertility/high-mortality countries but the United Nations produces TFR estimates for all countries post-1950. These data are subject to their own estimation, jiggering, and other post-processing that differ by country and by time period<sup>50,24</sup>. Due to the post-processing we present a brief analysis of the UN data here as we cannot determine if the errors we report here are due to the iTFR framework or due to the UN estimation process.

**Figure 5** reports the analysis for all three methods. Overall the methods produce estimated TFRs in good agreement with the UN estimates. All three formulations have a tendency to underestimate the UN TFR (**Fig. 5, j**). Most iTFR framework estimates are within 7% of the UN estimates, though some countries see considerably higher errors. These higher errors could be attributed to the post-processing undertaken by the UN.

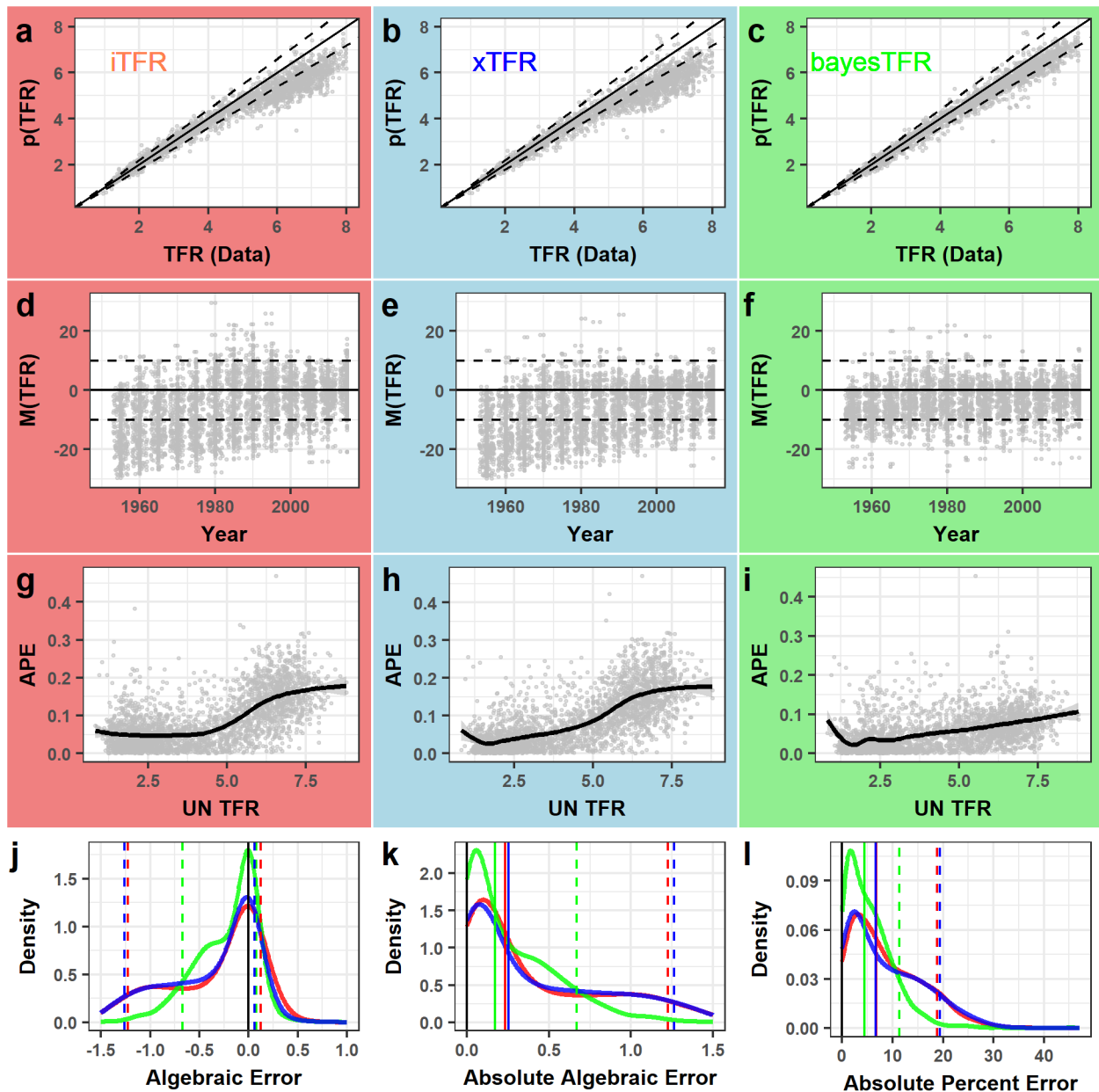


Figure 5: **United Nations TFR analysis using 2,613 country-periods.** (a, d, g) report the iTFR evaluation, (b, e, h) report the xTFR evaluation, and (c, f, i) report the bayesTFR. (d, e, f) report the algebraic error associated with each estimation method. (g, h, i) report the absolute percent error (APE) against the UN estimated TFR showing higher TFR in the UN data tends to produce higher errors, regardless of method. Overall the framework produces estimates in good agreement with the UN data in the majority of country-periods. Errors tend to be highest among high-fertility country-periods.

## References

1. Abel, G. J. and Sander, N. *Science* **343**(6178), 1520–1522 (2014).
2. Simini, F., Gonzalez, M. C., Maritan, A., and Barabasi, A.-L. *Nature* **484**(7392), 96–100 (2012). 10.1038/nature10856.
3. Dwyer-Lindgren, L., Bertozzi-Villa, A., Stubbs, R. W., Morozoff, C., Mackenbach, J. P., van Lenthe, F. J., Mokdad, A. H., and Murray, C. J. *JAMA Internal Medicine* (2017).
4. Gerland, P., Raftery, A. E., Ševčíková, H., Li, N., Gu, D., Spoorenberg, T., Alkema, L., Fosdick, B. K., Chunn, J., and Lalic, N. *Science* **346**(6206), 234–237 (2014).
5. Abel, G. J., Barakat, B., KC, S., and Lutz, W. *Proceedings of the National Academy of Sciences* **113**(50), 14294–14299 (2016).
6. Yule, G. U. *Journal of the Royal Statistical Society* **69**(1), 88–147 (1906).
7. Lutz, W. and KC, S. *Science* **333**(6042), 587–592 (2011).
8. Shenk, M. K., Towner, M. C., Kress, H. C., and Alam, N. *Proceedings of the National Academy of Sciences* **110**(20), 8045–8050 (2013).
9. Lesthaeghe, R. *Proceedings of the National Academy of Sciences* **111**(51), 18112–18115 (2014).
10. Myrskylä, M., Kohler, H.-P., and Billari, F. C. *Nature* **460**(7256), 741–743 (2009). 10.1038/nature08230.
11. Lee, R. and Mason, A. *Science* **346**(6206), 229–234 (2014).
12. Kaiser, J. *Science* **333**(6042), 548–549 (2011).
13. Conley, D., Laidley, T., Belsky, D. W., Fletcher, J. M., Boardman, J. D., and Domingue, B. W. *Proceedings of the National Academy of Sciences* **113**(24), 6647–6652 (2016).
14. Jones, J. H. and Tuljapurkar, S. *Proceedings of the National Academy of Sciences* **112**(29), 8982–8986 (2015).
15. Currie, J. and Schwandt, H. *Proceedings of the National Academy of Sciences* **111**(41), 14734–14739 (2014).
16. Bogue, D. and Palmore, J. *Demography* **1**(1), 316–338 (1964).
17. Hanson, W. R. *Wildlife Monographs* (9), 3–60 (1963).
18. Rele, J. *Fertility analysis through extension of stable population concepts*. Institute of International Studies, University of California, (1967).
19. Tuchfeld, B. S., Guess, L. L., and Hastings, D. W. *Demography* **11**(2), 195–205 (1974).

20. Hauer, M., Baker, J., and Brown, W. *PloS one* **8**(6), e67226 (2013).
21. Schmertmann, C. and Hauer, M. (2017).
22. Database, H. F. , Available at [www.fertilitydata.org](http://www.fertilitydata.org) (accessed on 1 May 2017).
23. Database, H. M. , Available at [www.mortality.org](http://www.mortality.org) or [www.humanmortality.de](http://www.humanmortality.de), (data downloaded on 1 May 2017).
24. Nations, U. (2015).
25. Bronikowski, A. M., Cords, M., Alberts, S. C., Altmann, J., Brockman, D. K., Fedigan, L. M., Pusey, A., Stoinski, T., Strier, K. B., and Morris, W. F. *Scientific data* **3** (2016).
26. Bronikowski, A. M., Cords, M., Alberts, S. C., Altmann, J., Brockman, D. K., Fedigan, L. M., Pusey, A., Stoinski, T., Strier, K. B., and Morris, W. F. 03/01/ (2016). Scientific Data.
27. Ha, J. C., Robinette, R. L., and Sackett, G. P. *American journal of primatology* **52**(4), 187–198 (2000).
28. Wich, S. A., Steenbeek, R., Sterck, E. H., Korstjens, A. H., Willems, E. P., and Van Schaik, C. P. *American Journal of Primatology* **69**(6), 641–651 (2007).
29. Jones, O. R., Scheuerlein, A., Salguero-Gómez, R., Camarda, C. G., Schaible, R., Casper, B. B., Dahlgren, J. P., Ehrlén, J., García, M. B., Menges, E. S., et al. *Nature* **505**(7482), 169 (2014).
30. Packer, C., Tatar, M., and Collins, A. *Nature* **392**(6678), 807 (1998).
31. Barlow, J. and Boveng, P. *Marine Mammal Science* **7**(1), 50–65 (1991).
32. Bronikowski, A. M., Altmann, J., Brockman, D. K., Cords, M., Fedigan, L. M., Pusey, A., Stoinski, T., Morris, W. F., Strier, K. B., and Alberts, S. C. *Science* **331**(6022), 1325–1328 (2011).
33. Hotz, V. J., Klerman, J. A., and Willis, R. J. *Handbook of population and family economics* **1**, 275–347 (1997).
34. Greenhalgh, S. *Situating fertility: Anthropology and demographic inquiry*. Cambridge University Press, (1995).
35. Paulson, R. J., Boostanfar, R., Saadat, P., Mor, E., Tourgeman, D. E., Slater, C. C., Francis, M. M., and Jain, J. K. *Jama* **288**(18), 2320–2323 (2002).
36. Woods, R. *The demography of victorian England and Wales*, volume 35. Cambridge University Press, (2000).
37. Sorichetta, A., Hornby, G. M., Stevens, F. R., Gaughan, A. E., Linard, C., and Tatem, A. J. *Scientific data* **2**, 150045 (2015).

38. Bongaarts, J. *Science* **282**(5388), 419–420 (1998).
39. Bocquet-Appel, J.-P. *Science* **333**(6042), 560–561 (2011).
40. Bagnall, R. S. and Frier, B. W. *The Demography of Roman Egypt*, volume 23. Cambridge University Press, (2006).
41. Jones, B., Oneill, B. C., McDaniel, L., McGinnis, S., Mearns, L. O., and Tebaldi, C. *Nature Clim. Change* **advance online publication** (2015). [rsquor].
42. Cincotta, R. P., Wisnewski, J., and Engelman, R. *Nature* **404**(6781), 990–992 (2000). 10.1038/35010105.
43. the Tree of Life database, D. T. D. A. , Available at [www.datlife.org](http://www.datlife.org), (data downloaded on 2 April 2018).
44. Wachter, K. *Essential Demographic Methods*. Harvard University Press, (2014).
45. United States Census Bureau. (2016).
46. Wilmoth, J., Zureick, S., Canudas-Romo, V., Inoue, M., and Sawyer, C. *Population studies* **66**(1), 1–28 (2012).
47. Carpenter, B., Gelman, A., Hoffman, M., Lee, D., Goodrich, B., Betancourt, M., Brubaker, M., Guo, J., Li, P., and Riddell, A. *Journal of Statistical Software* **76**(1), 1–32 (2017).
48. Stan Development Team. (2016). R package version 2.14.1.
49. R Core Team. *R: A Language and Environment for Statistical Computing*. R Foundation for Statistical Computing, Vienna, Austria, (2016).
50. Gerland, P. *Asian Population Studies* **10**(3), 274–303 (2014).